Neurobiology of Aging 36 (2015) 1601.e7–1601.e16

Contents lists available at ScienceDirect

Neurobiology of Aging

journal homepage: www.elsevier.com/locate/neuaging

The striatal long noncoding RNA Abhd11os is neuroprotective against an N-terminal fragment of mutant huntingtin in vivo

Laetitia Francelle [a,b,1], Laurie Galvan [a,b,1], Marie-Claude Gaillard [a,b], Fanny Petit [a,b], Benoît Bernay [c,d,e], Martine Guillermier [a,b], Gilles Bonvento [a,b], Noëlle Dufour [a,b], Jean-Marc Elalouf [c,d,e], Philippe Hantraye [a,b], Nicole Déglon [a,b], Michel de Chaldée [c,d,e], Emmanuel Brouillet [a,b,*]

[a] CEA, DSV, I²BM, Molecular Imaging Research Center (MIRCen), Fontenay-aux-Roses, France
[b] UMR 9199, CEA, CNRS, Université Paris-Sud, Neurodegenerative Diseases Laboratory, Fontenay-aux-Roses, France
[c] CEA, iBiTecS, Gif-sur-Yvette Cedex, France
[d] CNRS, FRE 3377, Gif-sur-Yvette Cedex, France
[e] Université Paris-Sud, FRE 3377, Gif-sur-Yvette Cedex, France

ARTICLE INFO

Article history:
Received 29 July 2014
Received in revised form 28 October 2014
Accepted 25 November 2014
Available online 18 December 2014

Keywords:
Huntington disease
Striatum
Neurodegeneration
Noncoding RNA
Neuroprotection
Gene regulation

ABSTRACT

A large number of gene products that are enriched in the striatum have ill-defined functions, although they may have key roles in age-dependent neurodegenerative diseases affecting the striatum, especially Huntington disease (HD). In the present study, we focused on Abhd11os, (called ABHD11-AS1 in human) which is a putative long noncoding RNA (lncRNA) whose expression is enriched in the mouse striatum. We confirm that despite the presence of 2 small open reading frames (ORFs) in its sequence, Abhd11os is not translated into a detectable peptide in living cells. We demonstrate that Abhd11os levels are markedly reduced in different mouse models of HD. We performed in vivo experiments in mice using lentiviral vectors encoding either Abhd11os or a small hairpin RNA targeting Abhd11os. Results show that Abhd11os overexpression produces neuroprotection against an N-terminal fragment of mutant huntingtin, whereas Abhd11os knockdown is protoxic. These novel results indicate that the loss lncRNA Abhd11os likely contribute to striatal vulnerability in HD. Our study emphasizes that lncRNA may play crucial roles in neurodegenerative diseases.

1. Introduction

Comprehensive analysis of the molecular "complexity" of the adult striatum has shown that many of the gene products preferentially expressed in this brain region have a poorly characterized function (Brochier et al., 2008). Among these "striatal" gene products, a nonnegligible fraction has never been studied experimentally. However, their enrichment in the striatum as compared with other brain regions, suggests they are involved in the functions of the striatum such as implementation of motor and cognitive behaviors. It is conceivable that they could also play a key role in the preferential degeneration of the striatum in a number of neurologic diseases and, as such, they constitute potential therapeutic targets.

Several disorders (e.g., Huntington disease [HD], Huntington disease type 2, multiple system atrophy, acute poisoning with mitochondrial toxins, inherited mitochondrial defects, and so forth) are primarily associated with striatal degeneration (Damiano et al., 2010) or secondarily lead to striatal dysfunctions (Parkinson's disease, L-dopa-induced dyskinesia, drug addiction, schizophrenia, among others). HD is a dominantly inherited disorder with an onset during adulthood. Symptoms include involuntary abnormal movements (chorea, dyskinesia, and dystonia), frontal cognitive deficits, and psychiatric disturbances (Harper, 1991; Walker, 2007). The disease is fatal approximately 15 years after the onset of symptoms. There is no effective treatment to slow the progression of HD. HD is caused by a mutation in the gene encoding the protein huntingtin (Htt) that consists in a CAG triplet repeat expansion translated into an abnormal polyglutamine (polyQ) tract within the N-terminal region of the

* Corresponding author at: CEA, DSV, I²BM, Molecular Imaging Research Center (MIRCen), Fontenay-aux-Roses, 92265, France. Tel.: 33 1 46 54 96 22; fax: 33 1 46 54 91 16.
E-mail address: emmanuel.brouillet@cea.fr (E. Brouillet).
[1] These authors are first co-authors. They equally contributed to the work.

0197-4580/
http://dx.doi.org/10.1016/j.neurobiolaging.2014.11.014

protein (The-Huntington's-Disease-Collaborative-Research-Group, 1993). This polyQ expansion produces a gain-of-function that is toxic to neurons through unclear mechanisms, but it is likely that many different cellular pathways are implicated (Roze et al., 2008). One major early event in HD is the alteration of transcription (Cha, 2007; Seredenina and Luthi-Carter, 2012). Other early alterations include intracellular signaling defects, axonal transport alterations (Borrell-Pages et al., 2006), deregulated autophagy (Winslow and Rubinsztein, 2008), defects in brain derived neurotrophic factor transcription, secretion, and transport (Zuccato and Cattaneo, 2014), perturbation of calcium homeostasis (Cowan and Raymond, 2006), and mitochondrial defects (Damiano et al., 2010).

Although mutant Htt (mHtt) protein is ubiquitously expressed in the brain, degeneration primarily affects the striatum (Tabrizi et al., 2013). This particular vulnerability may be conferred by factors that are enriched in the striatum (Brouillet et al., 2005; Desplats et al., 2006; Thomas, 2006). So far, only a limited list of gene products preferentially expressed in the striatum have been found to promote mHtt toxicity, notably the small GTPase Rhes (Subramaniam et al., 2009), the dopamine type 2 receptor (Benchoua et al., 2008; Charvin et al., 2005), and the RGS2 protein (Seredenina et al., 2011). Alternatively, striatum-enriched neuroprotective factors may be downregulated during HD pathogenesis. For instance, A(2A) adenosine receptors, whose expression is early impaired in HD (Blum et al., 2003), have been shown to be neuroprotective (Mievis et al., 2011). However, all striatal-specific gene products with reduced expression in HD have not an effect against mHtt (Galvan et al., 2012).

We previously reported that 2010001M06Rik transcript, one of those we have identified as striatal "markers", shows markedly reduced expression in the striatum of the R6/2 mouse model of HD (Brochier et al., 2008). It has been annotated as a long intergenic nonprotein coding RNA (LINC00035) by *in silico* analysis. It has been renamed ABHD11-AS1 in human and Abhd11os in mouse (for abhydrolase domain containing 11, opposite strand). The potential roles of long noncoding RNA in neurobiological regulatory mechanisms and neurologic and psychiatric diseases have been recently underlined (Tan et al., 2013; Wu et al., 2013). Thus, we aimed at exploring the potential role of Abhd11os in HD.

Here, we provide experimental evidence that Abhd11os is noncoding. We next examined its expression in the striatum of 2 additional mouse models of HD that are characterized by a slow progressing disease phenotype without major neurodegeneration. Finally, using lentiviral vectors, we tested whether overexpression or knock-down of Abhd11os could modify mHtt toxicity in the mouse striatum. Results indicate that Abhd11os is neuroprotective against mHtt in vivo.

2. Methods

2.1. Animals

Mice were housed in a temperature-controlled room maintained on a 12-hour light and/or dark cycle. Food and water were available ad libitum. All animal studies were conducted according to the French regulation (EU Directive 86/609—French Act Rural Code R 214-87 to 131). The animal facility was approved by veterinarian inspectors (authorization n°A 92-032-02) and complies with Standards for Humane Care and Use of Laboratory Animals of the Office of Laboratory Animal Welfare (OLAW—n°#A5826-01). All procedures received approval from the ethical committee. Adult male C57BL/6J mice (25 g each; Charles River, Saint Germain sur l'Arbresle, France) were used for lentiviral infections.

For endogenous Abhd11os messenger RNA (mRNA) levels study, we used the transgenic mouse model of HD generated and maintained in the FvB inbred background, the BACHD mice, that express full-length human mHtt from its own regulatory elements on a 240-kb BAC, which contains the intact 170-kb human htt locus plus about 20 kb of 5′ flanking genomic sequence and 50 kb of 3′. We used 9-month-old male BACHD mice for the study as previously described (Gray et al., 2008).

We also studied 13-month-old knock-in mice expressing chimeric mouse and/or human exon 1 containing 140 CAG repeats inserted in the murine Htt gene (KI140) and their littermate controls. KI140 colony was maintained by breeding heterozygotes KI140 males and females (Menalled et al., 2003). Mice were N3 (B6) on a 129 Sv × C57BL/6 J background. The resulting different genotypes mice were used for the study and showed no overt abnormalities.

Genotyping was determined from polymerase chain reaction (PCR) of tail snips taken at 10–15 days of age for BACHD and KI140 mice.

2.2. Lentiviral vector construction, production, and infection

DNA sequences coding for green fluorescent protein (GFP) and mouse Abhd11os (2010001M06rik) were cloned into the SIN-W-PGK lentiviral vector (LV) to generate LV-GFP and LV-Abhd11os, respectively (de Almeida et al., 2002). An Abhd11os-directed small hairpin RNA (shRNA) (target sequence: 5′ GGGATGAAGC-CATTGCTAA 3′) and a Luciferase-targeted shRNA (target sequence: 5′ CGTACGCGGAATACTTCGA 3′) were cloned into a bicistronic LV vector (Drouet et al., 2009), in such a way that the infected cells expressed the reporter protein GFP. The resulting constructs were designated as LV-shAbhd11os and LV-shLuc, respectively. The Abhd11os sequence targeted by the shRNA (GGGATGAAGC-CATTGCTAA) is located in the second exon of the Abhd11os gene. From the expressed sequence tag and complementary DNA (cDNA) sequences available in the public databases, this exon is present in all splice variants.

The lentiviral vectors expressing a wild-type Htt fragment (LV-Htt171-18Q), a mHtt fragment (LV-Htt171 82Q) or beta-galactosidase (LV-LacZ) have been described previously (Diguet et al., 2009; Faideau et al., 2010). Viral particles were produced as described elsewhere (Hottinger et al., 2000). The particle content of the viral batches was determined by enzyme-linked immunosorbent assay for the p24 antigen (Gentaur, Paris, France). LV-Htt171 18Q and LV-Htt171-82Q were used at a concentration of 150 ng/μL of p24, LV-Abhd11os, and LV-LacZ at a concentration of 100 ng/μL of p24. LV-shAbhd11os and LV-shLuc were used at a concentration of 100 ng/μL of p24. In experiments performed for PCR analysis, LV-GFP was mixed with LV-Abhd11os or LV-LacZ at a concentration of 50 ng/μL of p24. After being anesthetized (ketamine and/or xylazine), mice received a total volume of 2 μL of lentiviral suspension into the mouse striatum as previously reported (Faideau et al., 2010; Galvan et al., 2012), using the following stereotaxic coordinates: 1 mm anterior and 2 mm lateral to the bregma, at a depth of 2.7 mm from the dura, with the tooth bar set at 0.0 mm.

2.3. Histologic and cytological analyses

2.3.1. Brain processing

After deep anesthesia by intraperitoneal injection of a sodium pentobarbital solution (50 μg per gram of body weight), mice were transcardially perfused with 100 mL of phosphate buffer containing 4% paraformaldehyde at 8 mL/min. The brains were removed, postfixed overnight in the same solution, then cryoprotected by immersion in a 30% sucrose solution for 24 hours. Free-floating 30-μm-thick serial coronal sections throughout the striatum (i.e., 210-μm intersection space) were collected using a freezing sliding microtome (SM2400; Leica Microsystems, Wetzlar, Germany).

2.3.2. Immunohistochemistry

Sections were treated with 0.3% hydrogen peroxide for 1 hour, washed 3 times in phosphate-buffered saline (PBS), blocked in PBS containing 4.5% normal goat serum for 1 hour, then incubated overnight at 4 °C in PBS containing 3% normal goat serum, and one of the following antibodies: rabbit anti-DARPP 32 (Santa Cruz Biotechnology, Santa Cruz, CA; 1:1000), mouse anti-NeuN (Millipore, Molsheim, France; 1:200), rabbit anti-Ubiquitin (Wako Chemicals, Neuss, Germany; 1:1000), or mouse anti-hemagglutinin (HA; Covance, Princeton, NJ; 1:500). Sections were rinsed 3 times in PBS before incubation with the appropriate anti-IgG biotinylated antibody (Vector Laboratories, Burlingame, CA) at a 1:5000 dilution for 1 hour. Staining was visualized by the addition of avidin-biotinylated peroxidase and incubation with diaminobenzidine or Peroxidase Substrate Kit (Vector VIP) (Vector Laboratories) for 1 minute. For NeuN immunostaining, we used the M.O.M. immunodetection kit (Vector Laboratories). Stained sections were mounted on microscopic slides and cover slipped using Permount.

2.3.3. Quantitative histologic evaluation

The area of the striatal lesions resulting from LV-Htt171-82Q infection was delineated manually by identifying the border of the lesion (loss of DARPP-32 and NeuN immunolabelling). Lesion area was delineated using a 5× objective. Depending on the anteroposterior extension of the lesions, 3–8 coronal sections were analyzed for each mouse. Observation of sections and calculation of the surface of lesioned area were performed using a Leica DM6000 equipped with a motorized stage and an automated image acquisition and analysis system (Mercator software, Explora Nova, La Rochelle, France). The volume of the striatal lesion (V) was determined using the Cavalieri method (Damiano et al., 2013; Diguet et al., 2009; Galvan et al., 2012). The number of ubiquitin-positive inclusions was quantified as previously described (Damiano et al., 2013; Diguet et al., 2009; Galvan et al., 2012) with the following modifications: the intersection distance was 210 μm (i.e., one in every 7 sections was used), and observations were performed using a 10× objective on an Axioplan 2 Imaging microscope (Carl Zeiss, Le Pecq, France) equipped with a motorized stage and an automated image acquisition and analysis system (Mercator software, Explora Nova). With this set-up, objects with an apparent cross-sectional area >3 μm^2 (i.e., diameter > approximately 1 μm) could be reliably detected.

2.4. Real-time quantitative PCR

Adult mice were deeply anesthetized by intraperitoneal injection of a sodium pentobarbital solution (50 μg per gram of body weight) before decapitation. The brains were immediately removed and positioned in a coronal brain matrix (Ted Pella, Redding, CA).

For the quantification of overexpressed or downregulated Abhd11os mRNA levels, mice were infected with a mixture of LV-Abhd11os and LV-GFP or LV-shAbhd11os (bicistronic for GFP) alone. Injection of LV-LacZ and LV-shLuc were used as controls for viral load. The striatal region displaying fluorescence was dissected out using a circular punch (1.5 mm diameter) from 1-mm-thick fresh coronal brain sections visualized under a fluorescence binocular microscope (Leica). Total RNA extraction and real-time quantitative reverse transcription polymerase chain reaction (qRT-PCR) were performed as previously described (Drouet et al., 2009; Galvan et al., 2012), using the following primer sequences Abhd11os-U GGATTGCCTCGGACCTG and Abhd11os-L GCACCCGCTCTCGAAC. This pair of primers allows detection of all Abhd11os splice variants containing the intron.

Similar procedure was used for determination of Abhd11os RNA levels in BACHD mice and KI140 mice. In this latter case, expression levels were normalized to the geometric mean of the mRNAs (ΔCt) of 3 housekeeping genes (cyclophilin A [PPIA], hypoxanthine phosphoribosyltranferase [HPRT1], and beta-actin [ACTB]).

We also performed qRT-PCR to quantify Abhd11 RNA in the striatum after infection with LV-Abhd11os or its control. For this the following primer sequences Abhd11-U CACATTGGAGCCTTCATAGCAG and Abhd11-L CGCTTCCTTGACAACCGA.

2.5. Biochemical analysis

2.5.1. Cell culture

Human embryonic kidney 293T (HEK293T) cells were grown at 37 °C in 5% CO_2 in Dulbeco's modified Eagle's medium supplemented with 10% bovine calf serum, 1% L-glutamine, and antibiotics (50 units/mL penicillin and 50 μg/mL streptomycin).

HEK293T cells were transfected with recombinant Abhd11os vectors (coding the putative open reading frame 1 (ORF1) or ORF2 sequences—see Supplementary Fig.1) or equivalent amount of empty vector, using the calcium phosphate method. Putative ORF1 and ORF2 were subcloned from Abhd11os cDNA into pcDNA3 expression vector (PGK promoter). Six nucleotides were retained 5′ to the potential ATG start codon to preserve the endogenous context of translation initiation. A sequence coding for HA was introduced immediately 5′ to the stop codon. The resulting constructs have the following sequences (the putative coding sequence is in capital letters; the sequence encoding the HA tag is underlined):

ORF1: agagggATGAAGCCATTGCTAAGAAGCGCGCGGTGGAAGAGGAGCTGGACTCCTGTCGAGCCAGGCTGCGCACAGTGGAGGCTCAGCTGCTGGAGGTCCTGCAGGAGAAACGCCTACCCATACGACGTGCCTGACTACGCCTCCtga and ORF2: gaagacATGCAGCATATGGTTCGAGAGCGGGTGCGGAGTCAGCTGCAGGGAGAGCCCAGAGGCACCCTGGGAACACACGAGAACACAAGCCCGGGCAGAAGTTCCTGGATTCAACTCTCCCGGGGTCAGTGGGGGCGACGGTGGGCCTACCCATACGACGTGCCTGACTACGCCTCCtga.

Negative controls (ORF1ΔATG and ORF2ΔATG) were obtained by deleting the initial ATG codon and, for ORF2, by mutating the downstream ATG codon into CTG.

2.5.2. Western blotting

Transfected cultured cells were harvested 48 hours after transfection and lyzed in modified RIPA buffer: 50 mM Tris pH 8.0, 50 mM NaCl, 1 mM EDTA, 0.5% Triton-X100, 1% NP40, and protease inhibitor cocktail (Roche). Cell lysates were centrifuged at 13,000*g* for 20 minutes at 4 °C. Total protein concentration was tested with BCA kit (Pierce).

Equal amounts of total protein extract were subjected to sodium dodecyl sulfate poly-acrylamide gel electrophoresis in precast 4%–12% Bis-tris gel (NuPAGE Novex Bis-tris midi gel, 15wells, Life Technology) or in precast 4%–20% Bis-glycine gel (Thermo-Fisher) and transferred to nitrocellulose membranes. Blocked membranes (5% milk in TBS-0.1% Tween-20) were incubated with primary antibodies: HA (1:3000, mouse, Covance), actin (1:4000, rabbit, Sigma), active caspase-3 (1:800, mouse, Millipore, AB3623), and washed 3 times with TBS-0.1% Tween-20 for 10 minutes. Membranes were then labeled with secondary IgG-HRP antibodies raised against each corresponding primary antibody. After 3 washes, the membranes were incubated with Immun-Star WesternC kit (BioRad) according to the instructions of the supplier. Peroxidase activity was detected with camera system Fusion TX7 (Fisher scientific).

2.6. Statistical analysis

All data were expressed as means ± standard error of the mean (SEM). Unpaired Student *t* test was used for the

comparison between 2 groups. When more than 2 groups were compared, a 1-way analysis of variance with multiple comparisons using the post hoc Bonferroni test was carried out using commercially available software (StatView software, version 5.0, SAS Institute Inc, USA).

3. Results

3.1. Abhd11os RNA is not translated into a detectable peptide in living cells

ABHD11-AS1 RNA is an approximately 473-base-long transcript processed from 4 exons in human. ABHD11-AS1 and its mouse homolog Abhd1os contain 2 small potential ORFs (ORF1, 105 nucleotides and ORF2, 138 nucleotides in mouse), which are conserved across mammals. It has been shown that small ORFs can be translated into functional peptides in vivo (Galindo et al., 2007). Furthermore, Abhd11os transcript has been detected in the polysomal fraction of mouse striatal neurons (Supplementary Table 5 of Heiman et al., 2008). Thus, the possibility that Abhd11os may be coding for peptides could not be ruled out.

We therefore experimentally examined whether plasmids expressing either putative ORFs of Abhd11os (ORF1 or ORF2) tagged with C-terminal HA could generate a detectable peptide after transfection in HEK293T cells (Supplementary Fig. 1). As negative controls, ATG sites of each ORF were deleted (ORF1ΔATG and ORF2ΔATG). The transcripts of ORF1 and ORF2 (with or without ATG) could be readily detected by RT-qPCR 24 hours after transfection. As expected, Western blot analysis of protein extracts from cells transfected with ORF1ΔATG or ORF2ΔATG did not reveal the presence of an HA tag peptide (Supplementary Fig. 1). As positive control, in cells transfected with a plasmid coding the mouse striatal protein Dclk3 tagged with HA, a band at 90 kDa corresponding to full length mouse Dclk3 could be detected. In contrast, cell transfected with plasmids coding ORF1 or ORF2 did not reveal the presence of HA-containing low molecular weight peptides. Consistent with this, no specific fluorescent signal was observed in transfected cells subjected to immunofluorescence detection of the HA tag. These results support the hypothesis that, even when overexpressed, Abhd11os RNA does not lead to the production of a peptide. Thus as predicted, Abhd11os is a noncoding RNA.

3.2. Abhd11os expression is downregulated in HD mouse models

A major reduction in Abhd11os RNA levels was noted in the striatum of R6/2 mice, which express exon 1 of the human *HD* gene, containing 150 CAG repeats (the noncoding RNA Abhd11os was named 2010001M06rik; Brochier et al., 2008). To check that this loss of expression was not specific to the R6/2 model, we asked whether a similar change could be seen in the BACHD mouse model, which expresses human full-length mHtt (Gray et al., 2008). We also characterized Abhd11os RNA levels in a knock-in (KI140CAG) mouse model of HD (Menalled et al., 2003). A significant 33% reduction in Abhd11os RNA level was found in the striatum of 9-month-old BACHD mice as compared with control age-matched littermates (Fig. 1A). In heterozygous and homozygous KI140CAG mice, a significant approximately 70% reduction was found at 13 months of age (Fig. 1B) as compared with age-matched wild-type littermates (Fig. 1B).

3.3. Lentiviral vector approach to modulate Abhd11os expression in vivo

To study how Abhd11os expression could change the neurotoxicity of mHtt in striatal neurons in vivo, we chose to use a lentiviral model of HD. In this model, stereotaxic injection of LV encoding a short fragment of mHtt (LV-Htt171-82Q) produces a progressive loco-regional cell dysfunction and degeneration characterized by mHtt- and ubiquitin-containing inclusions, loss of markers linked to neuronal integrity, and astrogliosis within 6 weeks (Damiano et al., 2013; Faideau et al., 2010; Galvan et al., 2012; Ruiz and Deglon, 2012). This versatile model is particularly suitable to assess in vivo how mHtt toxicity can be modified by different proteins or RNA that can be co-expressed with the mutant protein using injection of a mixture of lentiviral vectors in the striatum (for a review Ruiz and Deglon, 2012).

For lentiviral-mediated overexpression of Abhd11os in vivo, we constructed a lentiviral vector expressing full-length mouse Abhd11os (LV-Abhd11os). To assess its efficiency, we injected it stereotaxically into the mouse striatum together with a lentiviral vector expressing GFP (LV-GFP). Six weeks after injection, brains were collected and the fluorescent region expressing GFP (and thus Abhd11os) was dissected out for RT-qPCR expression analysis. Results showed that LV-Abhd11os produced a 1.5-fold increase in Abhd11os expression compared with control (Fig. 2).

For Abhd11os knock-down, we designed a shRNA targeting Abhd11os. The efficacy of the shRNA was first tested in transfected

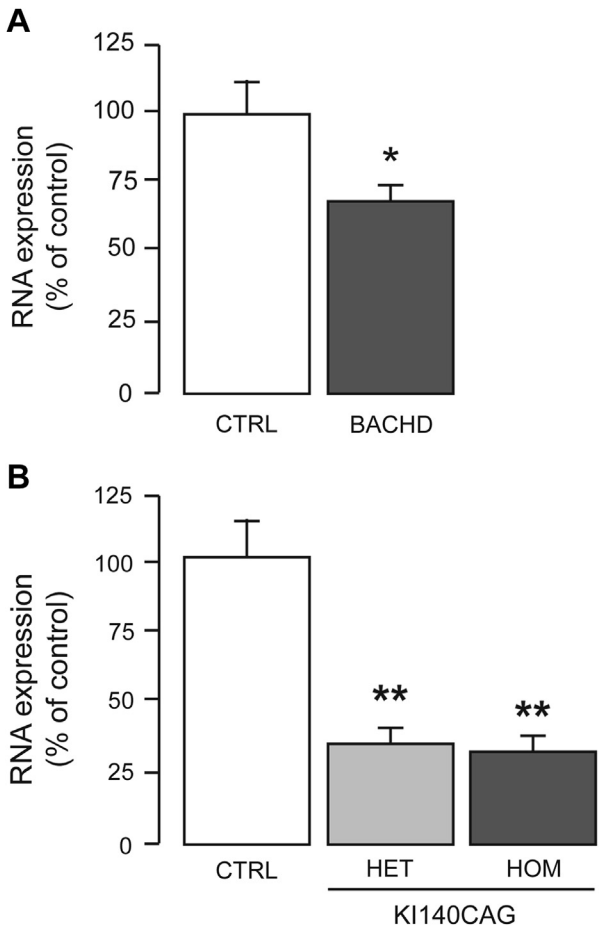

Fig. 1. Downregulated expression of Abhd11os in genetic mouse models of HD. Expression of Abhd11os was measured by RT-qPCR in 9-month-old BACHD mice (A) and 13-month-old KI140CAG (B). Controls (CTRL) are age-matched wild-type littermates. Results are presented as mean ± standard error of the mean. HET, heterozygous (140Q/+); HOM, homozygous (140Q/140Q) knock-in mice carrying an expanded CAG repeat. $^{*}p < 0.05$, n = 6 mice per group, unpaired Student *t* test; $^{**}p < 0.001$, n = 5 mice per group, 1-way ANOVA and Bonferroni post hoc. Abbreviations: ANOVA, analysis of variance; HD, Huntington disease.

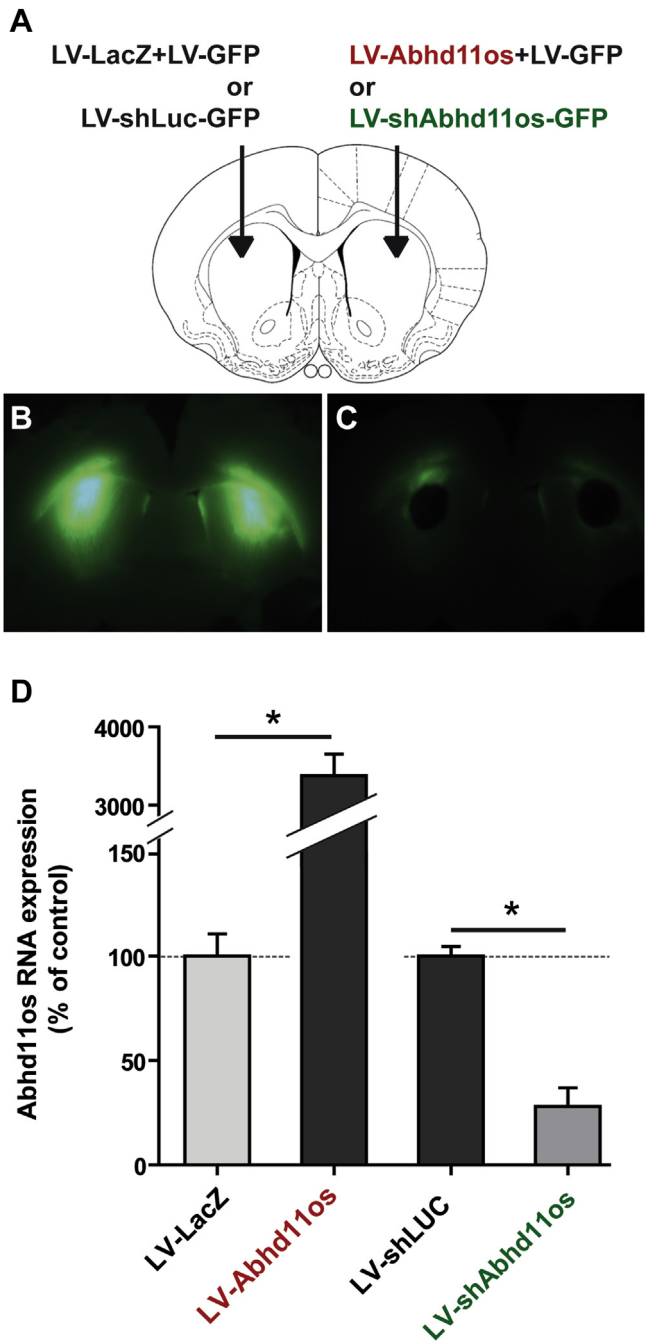

Fig. 2. Efficiency of the lentiviral vectors (LV) developed for Abhd11os overexpression and knock-down. (A) Mice were injected with LV-Abhd11os mixed with LV-GFP in a 4:1 ratio in the right striatum and with a lentiviral vector expressing beta-galactosidase (LV-LacZ; control) mixed with LV-GFP in the left striatum. A second group of mice was injected with LV-shAbhd11os-GFP (bicistronic construct also expressing GFP) in the right striatum and with a lentiviral vector expressing a shRNA directed against luciferase (LV-shLuc-GFP; control) in the left striatum. Six weeks later, the striatal regions expressing GFP (B) were dissected out from fresh slices using a punch (C) and analyzed by RT-qPCR (D). Results are expressed relative to controls as mean ± standard error of the mean (n = 5 to 7 mice per group). *$p < 0.0001$, paired Student t test. Abbreviations: GFP, green fluorescent protein; shRNA, small hairpin RNA.

HEK cells overexpressing Abhd11os. In this condition, expression of Abhd11os was reduced by approximately 85% by the shRNA targeting Abhd11os (Supplementary Fig. 1E). We inserted the corresponding DNA sequence into a bicistronic lentiviral backbone allowing co-expression with GFP (Drouet et al., 2009). The resulting lentiviral vector (LV-shAbhd11os) was stereotaxically injected in the striatum of adult C57Bl/6 mice. Six weeks after the infection, the brains were collected and fresh coronal slices encompassing the striatum were prepared. Because LV-shAbhd11os is bicistronic for the GFP, the transduced region was visible using a fluorescence binocular microscope and could be precisely resected and processed for RNA extraction. RT-qPCR analysis showed that LV-shAbhd11os produced a significant 75% reduction in the expression of endogenous Abhd11os as compared with control (Fig. 2).

The absence of toxicity of LV-Abhd11os and LV-shAbhd11os was verified by histologic evaluation 6 weeks after infection. Staining for NeuN and DARPP32, which are well-known markers of neuronal integrity in the striatum (de Almeida et al., 2002; Diguet et al., 2009; Drouet et al., 2009; Faideau et al., 2010; Galvan et al., 2012), revealed no degeneration in the infected striata (Figs. 3 and 4).

Thus, the LV-Abhd11os and LV-shAbhd11os are not neurotoxic per se and are effective to modulate Abhd11os expression in the mouse striatum.

3.4. Overexpression of Abhd11os protects against mHtt toxicity

To study the effects of Abhd11os overexpression on mHtt toxicity, we stereotaxically injected a mixed suspension of LV-Htt171-82Q and LV-Abhd11os into the mouse striatum. At 6 weeks post infection, LV-Htt171-82Q produced, a loss of NeuN and DARPP32 labeling in vicinity of the injection site, indicating overt neurodegeneration (Fig. 3). In separate experiments, we checked that co-infection with LV-LacZ (control) did not change the size of the lesion seen using NeuN immunohistochemistry as compared with LV-Htt171-82Q alone (not shown; mean ± SEM; NeuN, Htt171-82Q [n = 8 mice/group]: 0.440 ± 0.043 mm^3; Htt171-82Q/LacZ [n = 6 mice/group]: 0.526 ± 0.088 mm^3; Student t test, nonsignificant). Quantitative histologic evaluation using NeuN immunohistochemistry showed that the striatal lesions produced by a mixture of LV-Htt171-82Q and LV-Abhd11os were significantly smaller than those produced by LV-Htt171-82Q mixed with LV-LacZ (Fig. 3) (mean NeuN-depleted volume ± SEM; Htt171-82Q/Abhd11os [n = 6 mice/group]: 0.236 ± 0.062 mm^3; Htt171-82Q/LacZ [n = 9 mice/group]: 0.573 ± 0.086 mm^3; Student t test, $p < 0.02$]. In line with this, analysis of striatal degeneration using DARPP32 immunohistochemistry also showed that the overexpression of Abhd11os reduced the lesions produced by LV-Htt171-82Q (Fig. 3) (mean DARPP32-depleted volume ± SEM; Htt171-82Q/Abhd11os [n = 11 mice/group]: 0.289 ± 0.046 mm^3; Htt171-82Q/LacZ [n = 11 mice/group]: 0.438 ± 0.048 mm^3; Student t test, $p < 0.04$).

These results indicate that overexpression of Abhd11os can reduce the neurotoxicity of Htt171-82Q.

We then assessed the number and size of ubiquitin-positive nuclear inclusions in mice (Fig. 3) injected with a mixture of LV-Htt171-82Q and LV-Abhd11os or a mixture of LV-Htt171-82Q and LV-LacZ. Microscopic quantitative analysis of the sections processed by anti-ubiquitin-immunohistochemistry showed that overexpression of LV-Abhd11os changed neither the number of ubiquitin-containing inclusions (mean inclusion number ± SEM; Htt171-82Q/Abhd11os [n = 8 mice/group]: 10,189 ± 1597; Htt171-82Q/LacZ [n = 8 mice/group]: 11,141 ± 1330; Student t test, $p = 0.654$) nor their mean sizes (inclusion size, Htt171-82Q/Abhd11os [n = 8 mice/group]: 13.049 ± 1.266 μm^2; Htt171-82Q/LacZ [n = 8 mice/group]: 13.875 ± 1.059 μm^2; Student t test, $p = 0.624$).

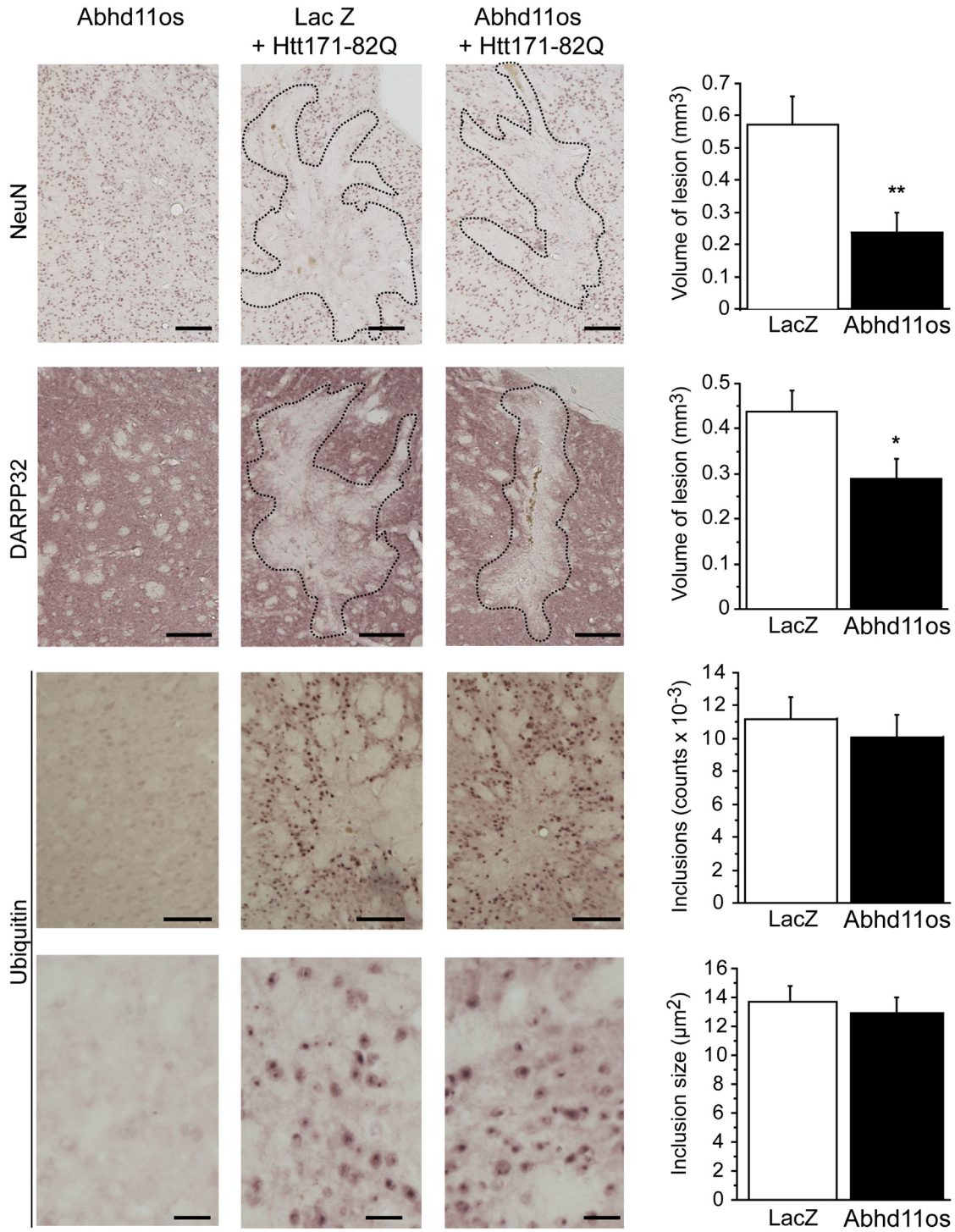

Fig. 3. Effect of the overexpression of Abhd11os on the toxicity induced by mHtt. Adult male mice received a bilateral intrastriatal injection of a mixture containing LV-Htt171-82Q with either LV-LacZ (LacZ, control) or LV-Abhd11os. Six weeks after infection, brains were processed for histologic evaluation using anti-DARPP32, anti-NeuN, and anti-ubiquitin-immunohistochemistry. Left panel: typical coronal mouse brain sections displaying representative areas with depleted staining. Right panel: histograms representing quantitative determination of the volume with depleted staining in the striatum. Results are expressed as mean ± standard error of the mean (n = 6–11 mice/group). $^{*}p < 0.05$; $^{**}p < 0.02$, unpaired Student *t* test. Scale bars: NeuN, DARPP32, 100 μm; ubiquitin, 50 μm; and (lower images) 20 μm. Abbreviations: LV, lentiviral vectors; mHtt, mutant huntingtin.

3.5. Knock-down of Abhd11os exacerbates mHtt toxicity

The effects of Abhd11os knock-down on mHtt toxicity were studied in the same mouse model. Co-infection with LV-Htt171-82Q and LV-sh Abhd11os produced NeuN-negative striatal lesions that were significantly larger than those produced by co-infection with LV-Htt171-82Q and control LV-shLuc (Fig. 4) (mean NeuN-depleted volume ± SEM; Htt171-82Q/shAbhd11os [n = 7 mice/group]: 0.541 ± 0.124 mm^3; Htt171-82Q/shLuc [n = 7]: 0.253 ± 0.043 mm^3; Student *t* test, $p < 0.05$), indicating that Abhd11os depletion may enhance mHtt toxicity. However, the volume of DARPP32-depleted area was similar in mice co-infected with LV-Htt171-82Q and

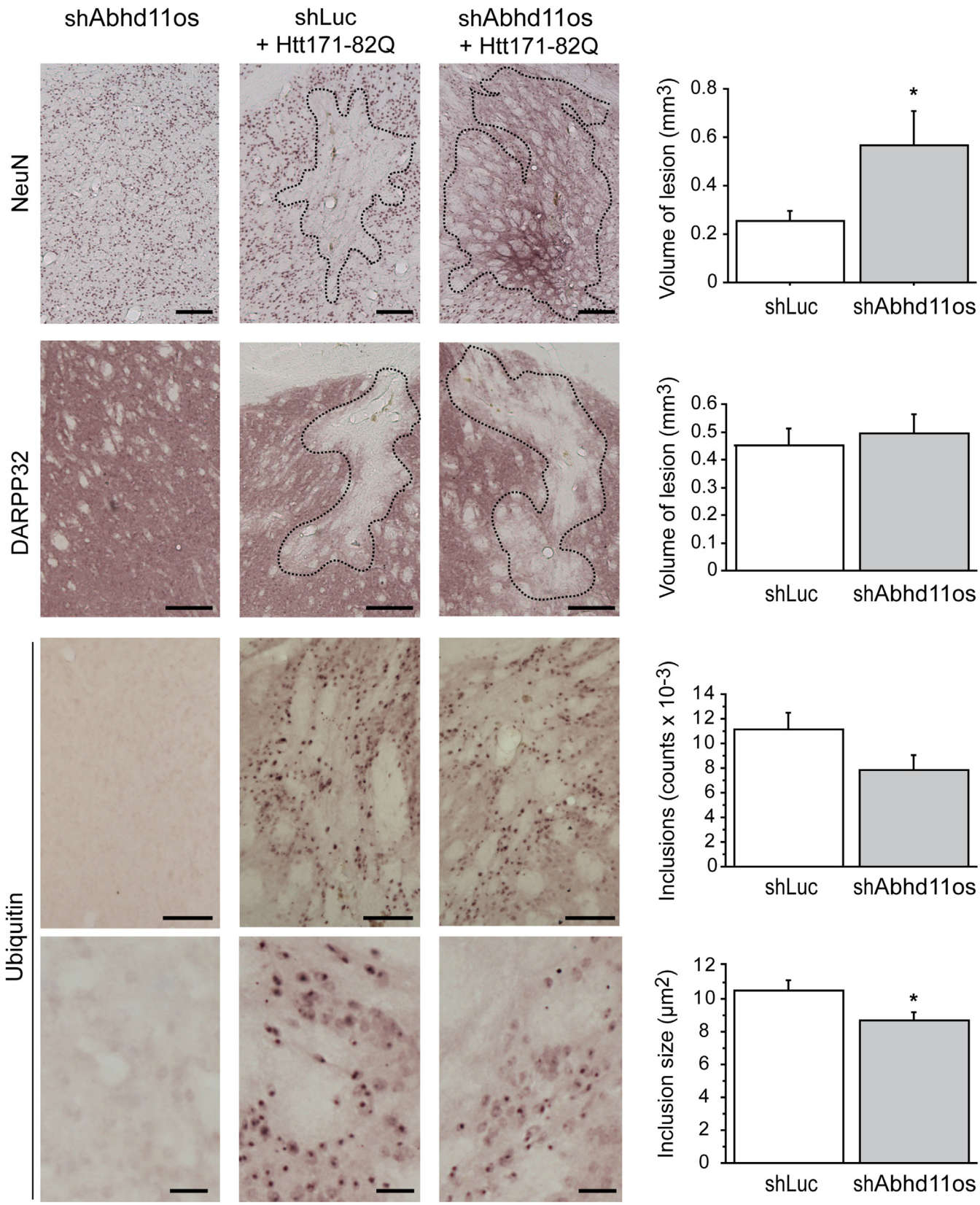

Fig. 4. Effect of the knock down of Abhd11os on the toxicity induced by mHtt. Adult male mice received a bilateral intrastriatal injection of a mixture containing LV-Htt171-82Q with either LV-shLuc (control) or LV-shAbhd11os. Six weeks after infection, brains were processed for histologic evaluation using anti-DARPP32, anti-NeuN, and anti-ubiquitin-immunohistochemistry. Left panel: typical coronal mouse brain sections displaying representative areas with depleted staining. Right panel: histograms representing quantitative determination of the volume with depleted staining in the striatum. Results are expressed as mean ± standard error of the mean (n = 7–12 mice/group). $^{*}p < 0.05$, unpaired Student *t* test. Scale bars: NeuN, DARPP32, 100 μm; ubiquitin, 50 μm; and (lower images) 20 μm. Abbreviations: LV, lentiviral vectors; mHtt, mutant huntingtin.

LV-shAbhd11os as compared with LV-shLuc (mean ± SEM; Htt171-82Q/shAbhd11os [n = 12 mice/group]: 0.488 ± 0.054 mm^3; Htt171-82Q/LacZ [n = 10 mice/group]: 0.454 ± 0.046 mm^3; Student *t* test, $p = 0.64$). The number of ubiquitin-positive nuclear inclusions in LV-shAbhd11os infected striata compared with control showed a trend toward reduction although it did not reach statistical significance (mean inclusion number ± SEM; Htt171-82Q/shAbhd11os [n = 8 mice/group]: 7861 ± 1283; Htt171-82Q/shLuc [n = 10 mice/group]: 11,221 ± 1497; Student *t* test, $p = 0.118$). The mean size of inclusions in LV-shAbhd11os infected striata was slightly (−18.5%) but significantly smaller as compared with LV-shLuc infected striata (Fig. 4) (mean inclusion size ± SEM, Htt171-82Q/shAbhd11os [n = 9 mice/group]: 8.661 ± 0.544 μm^2; Htt171-82Q/shLuc (n = 10 mice/group): 10.638 ± 0.630 μm^2; Student *t* test, $p < 0.04$).

Altogether, these results suggest that Abhd11os exerts a neuroprotective effect against the striatal toxicity of mHtt in vivo, whereas its downregulation exacerbates the toxicity of mHtt.

3.6. *Abhd11os does not directly downregulate expression of Abhd11 mRNA*

The underlying mechanism of the effect of Abhd11os toward mHtt toxicity is unknown. Because Abhd11os gene overlaps the antisense 3′UTR region of the Abhd11 gene, we asked whether Abhd11os could directly regulate Abhd11 mRNA expression through an antisense-like effect where Abhd11os hybridizing to Abhd11 mRNA and accelerating its degradation could negatively regulate Abhd11 expression. We performed qRT-PCR to quantify Abhd11 RNA in the striatum after infection with LV-Abhd11os or its control. Results showed that overexpression of Abhd11os produced a slight increase (+25) in Abhd11 mRNA expression (Supplementary Fig. 2). This indicated that Abhd11os did not directly downregulate Abhd11 mRNA.

4. Discussion

Different systematic studies aimed at providing a comprehensive view of the molecular "complexity" of the striatum have shown that many of the preferential gene products of this brain region have a totally unknown function. However, their particular presence in the striatum as compared with other brain region, suggests that they play a key role in striatal function such as motor behavior and cognition. Depending on the data sets considered and methods used, numbers can vary substantially, but a large number of gene products show preferential expression in the striatum. Using a SAGE-based method, we previously identified 120 gene products whose expression levels are at least 5 times higher in the striatum than in other brain regions (Brochier et al., 2008). Among these "striatal" gene products, a large proportion are poorly characterized (<100 entries in PubMed), especially in terms of neurobiological functions and/or roles and for a nonnegligible fraction of these gene products, experiments have never been reported (0 entry in PubMed). In comparison, well-known specific striatal gene products, considered as striatal markers, such as the phosphatase DARPP32 have hundreds of entries in public bibliographic databases.

In the present study, we focused on the newly identified striatal marker Abhd11os and found that its expression is significantly reduced in the striatum of 2 mouse models of HD that express full length Htt with a pathologic expansion (BACHD and KI140CAG), which is consistent with the major loss of Abhd11os, we previously found in the R6/2 model (Brochier et al., 2008). We asked whether experimental modification of Abhd11os expression in the mouse striatum could change the toxicity of mHtt. For this purpose, we designed lentiviral vectors encoding Abhd11os and a shRNA targeting Abhd11os. Results showed that these vectors were effective in increasing and reducing Abhd11os expression, respectively. The level of overexpression was limited (1.5-fold) using our system. Possibly, this suggests endogenous mechanisms of regulation, as Abhd11os has a weak basal RNA expression in healthy organisms. Indeed, using the very same strategy (same lentiviral vector backbone and promoter) for overexpression, we were able to express more strongly other recombinant transcripts such as mitochondrial complexes subunits and the striatal protein capucin (Damiano et al., 2013; Galvan et al., 2012).

To test the effects of Abhd11os on mHtt, we used a lentiviral model of HD in vivo, which is a highly flexible approach for the targeted overexpression of a disease-causing gene, with rapid and progressive phenotypes (Ruiz and Deglon, 2012). This HD model has already been used to test new experimental therapeutics targeting protein misfolding, mitochondrial defects, cell signaling, and mHtt itself (Damiano et al., 2013; Drouet et al., 2009; Galvan et al., 2012; Perrin et al., 2007, 2009; review in Ruiz and Deglon, 2012). Histologic evaluation showed that Abhd11os overexpression, although limited, produces a significant protective effect, reducing the volume of striatal lesions as seen using 2 different markers of striatal neuron integrity (NeuN and DARPP32). Conversely, the downregulation of Abhd11os was found to be protoxic, increasing the size of the striatal lesions produced by mHtt as seen using the neuronal marker NeuN. Lesions as seen by DARPP32 were not increased. The likely explanation for this is that at 6 weeks post-infection mHtt produced its maximal loss of DARPP32 neurons. In this model, loss of DARPP32 appears early after infection (de Almeida et al., 2002) and corresponds to a dysfunction of striatal neurons at first while NeuN immunoreactivity is spared. At later time points after infection, the loss of DARPP32 achieves its maximum, whereas NeuN loss which represents actual degeneration is still at its initial stage (Diguet et al., 2009). The number and size of ubiquitin (positive inclusions in the striatum, a neuropathologic hallmark of HD) were not changed by increased expression of Abhd11os. The shRNA targeting Abhd11os produced a significant but small (15%) reduction in the number and size of ubiquitin-positive inclusions. This small reduction might be attributed to the enhancement of neuronal cell death, leaving alive neurons that have the lowest levels of mHtt. These data suggest that the neuroprotective and/or protoxic effects resulting from the increased and/or decreased expression of Abhd11os are likely independent from a direct effect on mHtt expression and/or elimination and aggregation in neurons.

In parallel to the in vivo rescue experiments, we examined whether Abhd11os is truly a noncoding RNA (NCBI reference sequence: NR_026688). Our experiments showed that expression of the putative ORFs of Abhd11os in HEK293T cells could not reveal the existence of translated peptides. This correlates with the information provided by bioinformatics databases on the Abhd11os gene. Of course, we cannot rule out the possibility that the HA tag would be lost during transgene expression by the cells, but it would then be possible to detect this detached tag by Western blot, which was not the case. Thus it is highly probable that the neuroprotective effect of Abhd11os against mHtt is mediated by its RNA transcript.

Major efforts have been made to identify and explore the various roles of noncoding RNAs. For example, the ENCODE project has identified 9600 long noncoding RNAs (lncRNAs) (>200 nt), and some hints about their localization and roles in the cells have emerged (Cech and Steitz, 2014; Wu et al., 2013). Current hypotheses about the mechanisms of action of lncRNAs (Vucicevic et al., 2014) include interactions with proteins to bring along regulatory functions (Lai et al., 2013); and binding, guidance, and organization of chromatin domains to coordinate gene activation (Wang et al., 2011). They have been described to influence mRNA processing

and posttranscriptional regulation (Geisler and Coller, 2013) and to play direct and indirect roles on modulation of epigenetic regulation (Peschansky and Wahlestedt, 2014). The majority of lncRNAs expressed in the brain are thought to be brain region specific and could even be cell-specific and subcellular compartment-specific (ENCODE project). Increasing number of lncRNAs are being identified as interacting with genes or proteins implicated in neurodegenerative and psychiatric disorders, but only a few lncRNAs have so far been implicated in HD, as compared with other neurodegenerative diseases (Bhan and Mandal, 2014; Tan et al., 2013; Wu et al., 2013). Some lncRNAs seem to directly act on mHtt, as HTTAS_v1 whose overexpression specifically reduces endogenous Htt transcript levels (Chung et al., 2011), or DGCR5, a downstream target of repressor element-1 silencing transcription factor in HD that exacerbates the toxicity of mHtt (Johnson et al., 2009). Considering the diverse mechanisms proposed for lncRNA function (see as reviewfor example (Ulitsky and Bartel 2013), it would be tempting to think that Abhd11os could produce neuroprotective effects acting on transcriptional control, for example guiding chromatin remodeling proteins to target loci or acting with transcriptional factors, where the latter activate transcriptional program and Abhd11os could repress previous unstable transcriptional program. Or, it could also regulate gene expression of the downregulated or upregulated genes that are known to be modified by mHtt (see as reviews Seredenina and Luthi-Carter, 2012; Zuccato and Cattaneo, 2014). Abhd11os could also pair with other RNAs to trigger posttranscriptional regulation known to be altered in HD. Abhd11os could directly scaffold nuclear or cytoplasmic complexes. These different mechanisms are essential for the cells to function properly and may reduce damages induced by mHtt. If Abhd11os is implicated in some of these functions, its down regulation would amplify transcriptional dysregulation induced by mHtt, leading to cell dysfunction and death. As previously said, lincRNAs, as lncRNAs, are aimed to be brain region specific, cell-specific and subcellular compartment-specific, and depending on the function of Abhd11os, the elucidation of the mechanisms underlying the neuroprotective effects of Abhd11os overexpression against mHtt toxicity will require further studies. In this respect, it would be interesting to determine the localization of Abhd11os RNA in subcellular compartments with regard to functions that are most likely altered by mHtt. In particular, it would be tempting to speculate that Abhd11os could produce a neuroprotective effect by regulating the expression of a gene particularly important for neuronal survival. In line with this, we examined whether Abhd11os could directly regulate expression of Abhd11 mRNA, because Abhd11os gene is antisense with the 3′UTR region of Abhd11. Our results showed that overexpression of Abhd11os produces a slight increase in Abhd11 RNA expression and not a downregulation. In line with this, bioinformatics search indicates slight downregulation Abhd11 expression in HD mouse models. Thus, Abhd11os does not seem to directly regulate expression of Abhd11 mRNA levels.

In conclusion, because Abhd11os has a preferential expression in the striatum and its levels are early reduced in different HD models, it is possible that this downregulation may be involved in the preferential degeneration of the striatum in HD. Using an in vivo lentiviral model of HD, we showed that Abhd11os has a neuroprotective effect against mHtt. It should be emphasized that not all striatal markers deregulated in HD can modulate the toxicity of N-terminal fragments of mHtt in this model, and that even fewer candidates have been found to produce significant effects in both overexpression and downregulation experiments (Galvan et al., 2012; Ruiz and Deglon, 2012). The present study therefore identifies a new potential modifier of mHtt toxicity and as such may help in future works to define novel therapeutic targets to slow disease progression.

Disclosure statement

The authors of the present article declare to have no conflicts of interest.

Acknowledgements

This work was supported by annual recurrent funds from the Commissariat à l'Energie Atomique et aux Energies Alternatives (CEA) and Centre National de la Recherche Scientifique (CNRS). Laurie Galvan was supported by the Neuropôle de Recherche Francilien and the Fondation pour la Recherche Médicale. Laetitia Francelle was supported by the French Research Ministry. The research leading to these results has received funding from the European Community's Seventh Framework Program FP7/2007-2013 under grant agreement no. HEALTH-F5-2008-222925. The authors also received financial support from the IMAGEN European integrated project (EUR617037286).

Appendix A. Supplementary data

Supplementary data associated with this article can be found, in the online version, at http://dx.doi.org/10.1016/j.neurobiolaging.2014.11.014.

References

Benchoua, A., Trioulier, Y., Diguet, E., Malgorn, C., Gaillard, M.C., Dufour, N., Elalouf, J.M., Krajewski, S., Hantraye, P., Deglon, N., Brouillet, E., 2008. Dopamine determines the vulnerability of striatal neurons to the N-terminal fragment of mutant huntingtin through the regulation of mitochondrial complex II. Hum. Mol. Genet. 17, 1446–1456.

Bhan, A., Mandal, S.S., 2014. Long noncoding RNAs: emerging stars in gene regulation, epigenetics and human disease. ChemMedChem 9, 1932–1956.

Blum, D., Hourez, R., Galas, M.C., Popoli, P., Schiffmann, S.N., 2003. Adenosine receptors and Huntington's disease: implications for pathogenesis and therapeutics. Lancet Neurol. 2, 366–374.

Borrell-Pages, M., Zala, D., Humbert, S., Saudou, F., 2006. Huntington's disease: from huntingtin function and dysfunction to therapeutic strategies. Cell Mol. Life Sci. 63, 2642–2660.

Brochier, C., Gaillard, M.C., Diguet, E., Caudy, N., Dossat, C., Segurens, B., Wincker, P., Roze, E., Caboche, J., Hantraye, P., Brouillet, E., Elalouf, J.M., de Chaldee, M., 2008. Quantitative gene expression profiling of mouse brain regions reveals differential transcripts conserved in human and affected in disease models. Physiol. Genomics 33, 170–179.

Brouillet, E., Jacquard, C., Bizat, N., Blum, D., 2005. 3-Nitropropionic acid: a mitochondrial toxin to uncover physiopathological mechanisms underlying striatal degeneration in Huntington's disease. J. Neurochem. 95, 1521–1540.

Cech, T.R., Steitz, J.A., 2014. The noncoding RNA revolution-trashing old rules to forge new ones. Cell 157, 77–94.

Cha, J.H., 2007. Transcriptional signatures in Huntington's disease. Prog. Neurobiol. 83, 228–248.

Charvin, D., Vanhoutte, P., Pages, C., Borrelli, E., Caboche, J., 2005. Unraveling a role for dopamine in Huntington's disease: the dual role of reactive oxygen species and D2 receptor stimulation. Proc. Natl. Acad. Sci. U. S. A. 102, 12218–12223.

Chung, D.W., Rudnicki, D.D., Yu, L., Margolis, R.L., 2011. A natural antisense transcript at the Huntington's disease repeat locus regulates HTT expression. Hum. Mol. Genet. 20, 3467–3477.

Cowan, C.M., Raymond, L.A., 2006. Selective neuronal degeneration in Huntington's disease. Curr. Top Dev. Biol. 75, 25–71.

Damiano, M., Diguet, E., Malgorn, C., D'Aurelio, M., Galvan, L., Petit, F., Benhaim, L., Guillermier, M., Houitte, D., Dufour, N., Hantraye, P., Canals, J.M., Alberch, J., Delzescaux, T., Deglon, N., Beal, M.F., Brouillet,, E., 2013. A role of mitochondrial complex II defects in genetic models of Huntington's disease expressing N-terminal fragments of mutant huntingtin. Hum. Mol. Genet. 22, 3869–3882.

Damiano, M., Galvan, L., Deglon, N., Brouillet, E., 2010. Mitochondria in Huntington's disease. Biochim. Biophys. Acta 1802, 52–61.

de Almeida, L.P., Ross, C.A., Zala, D., Aebischer, P., Deglon, N., 2002. Lentiviral-mediated delivery of mutant huntingtin in the striatum of rats induces a selective neuropathology modulated by polyglutamine repeat size, huntingtin expression levels, and protein length. J. Neurosci. 22, 3473–3483.

Desplats, P.A., Kass, K.E., Gilmartin, T., Stanwood, G.D., Woodward, E.L., Head, S.R., Sutcliffe, J.G., Thomas, E.A., 2006. Selective deficits in the expression of striatal-enriched mRNAs in Huntington's disease. J. Neurochem. 96, 743–757.

Diguet, E., Petit, F., Escartin, C., Cambon, K., Bizat, N., Dufour, N., Hantraye, P., Deglon, N., Brouillet, E., 2009. Normal aging modulates the neurotoxicity of mutant huntingtin. PLoS One 4, e4637.
Drouet, V., Perrin, V., Hassig, R., Dufour, N., Auregan, G., Alves, S., Bonvento, G., Brouillet, E., Luthi-Carter, R., Hantraye, P., Deglon, N., 2009. Sustained effects of nonallele-specific Huntingtin silencing. Ann. Neurol. 65, 276–285.
Faideau, M., Kim, J., Cormier, K., Gilmore, R., Welch, M., Auregan, G., Dufour, N., Guillermier, M., Brouillet, E., Hantraye, P., Deglon, N., Ferrante, R.J., Bonvento, G., 2010. In vivo expression of polyglutamine-expanded huntingtin by mouse striatal astrocytes impairs glutamate transport: a correlation with Huntington's disease subjects. Hum. Mol. Genet. 19, 3053–3067.
Galindo, M.I., Pueyo, J.I., Fouix, S., Bishop, S.A., Couso, J.P., 2007. Peptides encoded by short ORFs control development and define a new eukaryotic gene family. PLoS Biol. 5, e106.
Galvan, L., Lepejova, N., Gaillard, M.C., Malgorn, C., Guillermier, M., Houitte, D., Bonvento, G., Petit, F., Dufour, N., Hery, P., Gerard, M., Elalouf, J.M., Deglon, N., Brouillet, E., de Chaldee, M., 2012. Capucin does not modify the toxicity of a mutant Huntingtin fragment in vivo. Neurobiol. Aging 33, 1845 e1845–1846.
Geisler, S., Coller, J., 2013. RNA in unexpected places: long non-coding RNA functions in diverse cellular contexts. Nat. Rev. Mol. Cell. Biol. 14, 699–712.
Gray, M., Shirasaki, D.I., Cepeda, C., Andre, V.M., Wilburn, B., Lu, X.H., Tao, J., Yamazaki, I., Li, S.H., Sun, Y.E., Li, X.J., Levine, M.S., Yang, X.W., 2008. Full-length human mutant huntingtin with a stable polyglutamine repeat can elicit progressive and selective neuropathogenesis in BACHD mice. J. Neurosci. 28, 6182–6195.
Harper, P.S. (1991). Huntington's Disease.
Heiman, M., Schaefer, A., Gong, S., Peterson, J.D., Day, M., Ramsey, K.E., Suarez-Farinas, M., Schwarz, C., Stephan, D.A., Surmeier, D.J., Greengard, P., Heintz, N., 2008. A translational profiling approach for the molecular characterization of CNS cell types. Cell 135, 738–748.
Hottinger, A.F., Azzouz, M., Deglon, N., Aebischer, P., Zurn, A.D., 2000. Complete and long-term rescue of lesioned adult motoneurons by lentiviral-mediated expression of glial cell line-derived neurotrophic factor in the facial nucleus. J. Neurosci. 20, 5587–5593.
Johnson, R., Teh, C.H., Jia, H., Vanisri, R.R., Pandey, T., Lu, Z.H., Buckley, N.J., Stanton, L.W., Lipovich, L., 2009. Regulation of neural macroRNAs by the transcriptional repressor REST. RNA 15, 85–96.
Lai, F., Orom, U.A., Cesaroni, M., Beringer, M., Taatjes, D.J., Blobel, G.A., Shiekhattar, R., 2013. Activating RNAs associate with mediator to enhance chromatin architecture and transcription. Nature 494, 497–501.
Menalled, L.B., Sison, J.D., Dragatsis, I., Zeitlin, S., Chesselet, M.F., 2003. Time course of early motor and neuropathological anomalies in a knock-in mouse model of Huntington's disease with 140 CAG repeats. J. Comp. Neurol. 465, 11–26.
Mievis, S., Blum, D., Ledent, C., 2011. A2A receptor knockout worsens survival and motor behaviour in a transgenic mouse model of Huntington's disease. Neurobiol. Dis. 41, 570–576.
Perrin, V., Dufour, N., Raoul, C., Hassig, R., Brouillet, E., Aebischer, P., Luthi-Carter, R., Deglon, N., 2009. Implication of the JNK pathway in a rat model of Huntington's disease. Exp. Neurol. 215, 191–200.
Perrin, V., Regulier, E., Abbas-Terki, T., Hassig, R., Brouillet, E., Aebischer, P., Luthi-Carter, R., Deglon, N., 2007. Neuroprotection by Hsp104 and Hsp27 in lentiviral-based rat models of Huntington's disease. Mol. Ther. 15, 903–911.
Peschansky, V.J., Wahlestedt, C., 2014. Non-coding RNAs as direct and indirect modulators of epigenetic regulation. Epigenetics 9, 3–12.
Roze, E., Saudou, F., Caboche, J., 2008. Pathophysiology of Huntington's disease: from huntingtin functions to potential treatments. Curr. Opin. Neurol. 21, 497–503.
Ruiz, M., Deglon, N., 2012. Viral-mediated overexpression of mutant huntingtin to model HD in various species. Neurobiol. Dis. 48, 202–211.
Seredenina, T., Gokce, O., Luthi-Carter, R., 2011. Decreased striatal RGS2 expression is neuroprotective in Huntington's disease (HD) and exemplifies a compensatory aspect of HD-induced gene regulation. PLoS One 6, e22231.
Seredenina, T., Luthi-Carter, R., 2012. What have we learned from gene expression profiles in Huntington's disease? Neurobiol. Dis. 45, 83–98.
Subramaniam, S., Sixt, K.M., Barrow, R., Snyder, S.H., 2009. Rhes, a striatal specific protein, mediates mutant-huntingtin cytotoxicity. Science 324, 1327–1330.
Tabrizi, S.J., Scahill, R.I., Owen, G., Durr, A., Leavitt, B.R., Roos, R.A., Borowsky, B., Landwehrmeyer, B., Frost, C., Johnson, H., Craufurd, D., Reilmann, R., Stout, J.C., Langbehn, D.R., Investigators, T.-H., 2013. Predictors of phenotypic progression and disease onset in premanifest and early-stage Huntington's disease in the TRACK-HD study: analysis of 36-month observational data. Lancet Neurol. 12, 637–649.
Tan, L., Yu, J.T., Hu, N., Tan, L., 2013. Non-coding RNAs in Alzheimer's disease. Mol. Neurobiol. 47, 382–393.
The-Huntington's-Disease-Collaborative-Research-Group, 1993. A novel gene containing a trinucleotide repeat that is expanded and unstable on Huntington's disease chromosomes. The Huntington's Disease Collaborative Research Group. Cell 72, 971–983.
Thomas, E.A., 2006. Striatal specificity of gene expression dysregulation in Huntington's disease. J. Neurosci. Res. 84, 1151–1164.
Ulitsky, I., Bartel, D.P., 2013. lincRNAs: genomics, evolution, and mechanisms. Cell 154, 26–46.
Vucicevic, D., Schrewe, H., Orom, U.A., 2014. Molecular mechanisms of long ncRNAs in neurological disorders. Front. Genet. 5, 48.
Walker, F.O., 2007. Huntington's disease. Lancet 369, 218–228.
Wang, K.C., Yang, Y.W., Liu, B., Sanyal, A., Corces-Zimmerman, R., Chen, Y., Lajoie, B.R., Protacio, A., Flynn, R.A., Gupta, R.A., Wysocka, J., Lei, M., Dekker, J., Helms, J.A., Chang, H.Y., 2011. A long noncoding RNA maintains active chromatin to coordinate homeotic gene expression. Nature 472, 120–124.
Winslow, A.R., Rubinsztein, D.C., 2008. Autophagy in neurodegeneration and development. Biochim. Biophys. Acta 1782, 723–729.
Wu, P., Zuo, X., Deng, H., Liu, X., Liu, L., Ji, A., 2013. Roles of long noncoding RNAs in brain development, functional diversification and neurodegenerative diseases. Brain Res. Bull. 97, 69–80.
Zuccato, C., Cattaneo, E., 2014. Huntington's disease. Handb. Exp. Pharmacol. 220, 357–409.